



**Extensive Characterization of the 1 mm PIT Nb<sub>3</sub>Sn strand  
for the 13-T FRESCA2 Magnet**

B. Bordini<sup>1</sup>, L. Bottura<sup>1</sup>, G. Mondonico<sup>2</sup>, L. Oberli<sup>1</sup>, D. Richter<sup>1</sup>, B. Seeber<sup>2</sup>,  
C. Senatore<sup>2</sup>, E. Takala<sup>1</sup>, D. Valentinis<sup>1</sup>  
1 CERN, Geneva, Switzerland  
2 University of Geneva, Geneva, Switzerland

**Abstract**

In the framework of the EuCARD program, CERN is participating in the development of a 13 T 100-mm-aperture dipole magnet to upgrade the superconducting cable test facility FRESCA at CERN. The conductor candidates for building this magnet are two 1-mm Nb<sub>3</sub>Sn strands: the Powder In Tube (PIT) produced by Bruker-EAS and the 132/169 RRP by Oxford Superconducting Technology (OST). Recently the PIT strand has been extensively characterized by CERN in collaboration with the University of Geneva (UniGe). The critical current dependence on the magnetic field and on the axial strain  $\varepsilon$  has been measured at different temperatures. Furthermore, the strand magnetization has been measured at different temperature using a vibrating sample magnetometer. Finally the magneto-thermal stability of this strand was studied by measuring the quench current between 0 T and 12 T at 1.9 K and 4.3 K. The experimental results are compared with an optimized scaling law for the critical current of Nb<sub>3</sub>Sn strands. In this paper the results obtained for the PIT strand are summarized and discussed.



# Extensive Characterization of the 1 mm PIT Nb<sub>3</sub>Sn strand for the 13-T FRESCA2 Magnet

B. Bordini, L. Bottura, G. Mondonico, L. Oberli, D. Richter, B. Seeber,  
C. Senatore, E. Takala, D. Valentinis

**Abstract**— In the framework of the EuCARD program, CERN is participating in the development of a 13 T 100-mm-aperture dipole magnet to upgrade the superconducting cable test facility FRESCA at CERN. The conductor candidates for building this magnet are two 1-mm Nb<sub>3</sub>Sn strands: the Powder In Tube (PIT) produced by Bruker-EAS and the 132/169 RRP by Oxford Superconducting Technology (OST). Recently the PIT strand has been extensively characterized by CERN in collaboration with the University of Geneva (UniGe). The critical current dependence on the magnetic field and on the axial strain  $\epsilon$  has been measured at different temperatures. Furthermore, the strand magnetization has been measured at different temperature using a vibrating sample magnetometer. Finally the magneto-thermal stability of this strand was studied by measuring the quench current between 0 T and 12 T at 1.9 K and 4.3 K. The experimental results are compared with an optimized scaling law for the critical current of Nb<sub>3</sub>Sn strands. In this paper the results obtained for the PIT strand are summarized and discussed.

**Index Terms**—Nb<sub>3</sub>Sn, PIT, Critical Current, Scaling Law

## I. INTRODUCTION

CERN has started an extensive research program to develop next generation accelerator magnets based on the high critical current density,  $J_c$ , Nb<sub>3</sub>Sn conductor [1]-[3]. Within this high field magnet program and in the framework of an European collaboration (EuCARD [2]), CERN is participating in the development of a 13-T 100-mm-aperture dipole magnet to upgrade the superconducting cable test facility FRESCA at CERN [4], [5]. At present the best conductor candidates for building this magnet are the 1 mm Nb<sub>3</sub>Sn Powder In Tube (PIT) strand produced by Bruker-EAS and the 1-mm 132/169 RRP strand by Oxford Superconducting Technology (OST). Recently the PIT strand has been extensively characterized by CERN in collaboration with the University of Geneva (UniGe). The critical current

dependence on the magnetic field (between 12 T and 19 T) and on the axially applied strain  $\epsilon$  (between -0.8 % and 0.5 %) at 4.2 K and 6.5 K has been investigated by testing few strand samples at UniGe. Furthermore, in order to study the magneto-thermal stability of this strand, quench current measurements have been performed at CERN between 0 T and 12 T at 1.9 K and 4.3 K. Finally the strand magnetization up to 10.5 T has been measured at different temperature (4.2 K, 6.5 K and 10 K), using a vibrating sample magnetometer, to assess the critical current density in the temperature and field range where transport current measurements were not available. The experimental results are compared with a scaling law for the critical current of Nb<sub>3</sub>Sn strands. In this paper the results obtained for the PIT strand are summarized and discussed, and the reference performance is documented for magnet design purposes.

## II. SAMPLES PREPARATION

The conductor characterized in this study is a 1-mm Nb<sub>3</sub>Sn PIT strand with 192 round superconducting sub-elements and a copper to non-copper ratio equal to 1.22, see Fig. 1. This conductor was appositely developed by Bruker-EAS for the FRESCA2 magnet; the round sub-elements ( $\varnothing \sim 50 \mu\text{m}$ ) were introduced to reduce the critical current degradation caused by the mechanical deformations experienced by the strand during cabling.

All the measured samples were prepared using adjacent strand piece lengths that were reacted in vacuum atmosphere. The heat treatment cycle was the following: 120 hours at 620 °C, 90 hours at 650 °C (the temperature was ramped up and down at 50 °C/hr).

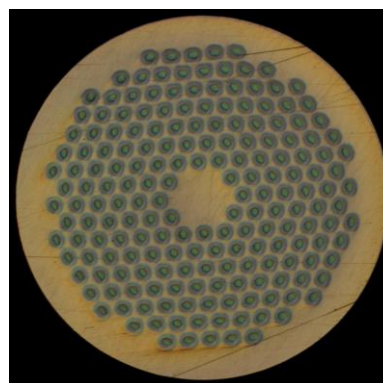


Fig. 1. Cross section of a reacted 1 mm PIT with 192 round superconducting sub-elements.

Manuscript received 12 September 2011.

B. Bordini, L. Bottura, L. Oberli, D. Richter, E. Takala and D. Valentinis are with CERN – Technology Department, Geneva 23, 1211 CH; (phone: +41-22-767-3049; fax: +41-22-767-6300; e-mail: [bernardo.bordini@cern.ch](mailto:bernardo.bordini@cern.ch)).

G. Mondonico, B. Seeber and C. Senatore are with University of Geneva.

For the critical current versus axial strain, six 1.10-m-long samples have been prepared: four were used for measurements at 4.2 K and two for measurements at 6.5 K. The samples have been heat treated on an oxidized stainless steel support ( $\varnothing = 39$  mm) to prevent sticking of the superconducting wire. During the heat treatment, the conductor is kept in position on the mandrel by a machined groove and an external tube. Such an arrangement allows the conductor to move axially. After the heat treatment the samples were carefully mounted on the Walter Spring (WASP) sample holder.

For the critical and stability current measurements all the sample were wound, reacted and tested on grooved cylindrical Ti-6Al-4V alloy barrels (ITER barrel). Two sets of samples were prepared: one based on a ‘virgin’ strand and the other on a ‘rolled’ strand that was mechanically deformed to study the effects of macroscopic mechanical deformations. In particular the strand, before being wound on the barrel, was rolled in such a way to create two opposite flat surfaces whose distance was 90% of the strand diameter. Two sets (‘virgin’ and ‘rolled’) of samples, each composed of three 11-cm-long straight wires, were also prepared for the measurements of the Residual Resistivity Ratio (RRR) of the stabilizing copper. For the magnetization measurements a 5-mm-long sample was cut from one of the ‘virgin’ RRR samples.

### III. STRAND MEASUREMENTS

#### A. Magnetization

The magnetization measurements were performed up to 10.5 T at three different temperatures: 4.2 K, 6.5 K and 10 K in a Vibrating Sample Magnetometer (VSM) at CERN. These measurements were used to determine the field and temperature dependence of the critical current density. In particular the magnetization measurements were used to find the optimal  $p$ ,  $q$  and  $T_{c0}$  parameters in the pinning force model used by CERN and the ITER project [6]:

$$F_p = J_c \times B = C s(\varepsilon) (1-t^{1.52}) (1-t^2) b^p (1-b)^q \quad (1)$$

where  $t$  and  $b$  are respectively the reduced temperature and field :  $t=T/T_c(0,\varepsilon)$ ;  $b=B/B_{c2}^*(T,\varepsilon)$ .

From the data at a certain temperature, the magnetization amplitude  $\Delta M$  was calculated in the field region where the field was fully penetrated. In this field region and for the considered wire, where each sub-element acts as one filament that is electrically decoupled from the others, the magnetization amplitude times the applied field is proportional to the pinning force  $F_p$ . Hence by fitting this quantity, the Kramer field  $B_{c2}^*$  at the three different temperatures was determined imposing in Eq. (1),  $p=0.5$  and  $q=2$ . Then by fitting the only data at 4.2 K and using the  $B_{c2}^*$  just calculated, the optimal  $p$  and  $q$  parameters for the pinning force were found. The values are close to those proposed by Kramer,  $p=0.453$  and  $q=1.90$ . Fig. 3 shows the normalized pinning force derived from the magnetization measurements at the 3 different temperatures together with the pinning force scaling law using the optimal  $p$  and  $q$  parameters. The measurements are in very good agreement with the pinning model.

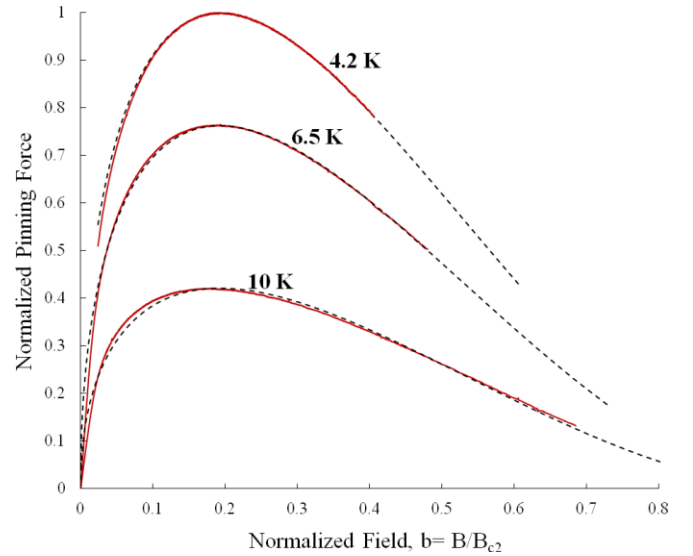


Fig. 2. Normalized pinning force at different temperatures derived from magnetization measurements. The normalization is done with respect to the maximum pinning force at 4.2 K. The dashed lines represent the pinning force model while the continuous lines represent the data from the magnetization measurements.

The  $T_c(0, \varepsilon_{Th})$ , where  $\varepsilon_{Th}$  is the thermally induced strain in the  $Nb_3Sn$  of the magnetization sample due to the different constituents of the wire, was then calculated using the  $B_{c2}^*$  values at the three temperatures together with the following formula [6]:

$$B_{c2}^*(T, \varepsilon) = B_{c20max}^* s(\varepsilon) (1-t^{1.52}) \quad (2)$$

The  $T_c(0, \varepsilon_{Th})$  was estimated at 16.1 K.

Finally the  $T_{c0max}$  was calculated using the following equation:

$$T_c^*(0, \varepsilon) = T_{c0max}^* [s(\varepsilon)]^{\frac{1}{3}} \quad (3)$$

and assuming  $s(\varepsilon_{Th}) \sim B_{c2}^*(4.2 K, \varepsilon_{Th}) / B_{c2max}^*(4.2 K)$ . Where  $B_{c2}^*(4.2 K, \varepsilon_{Th})=25.4$  T is derived from the magnetization measurements and  $B_{c2max}^*(4.2 K)=26.6$  T from the critical current measurements versus applied axial strain presented in the next section. The  $T_{c0max}$  was estimated at 16.3 K.

#### B. Critical Current vs. Axial Strain

In order to study the dependence of the critical current on the strain, critical current measurements versus applied axial strain were performed at the University of Geneva using a WASP sample holder. The measurements were carried out in the reversible region of the applied strain (between  $-0.785\%$  and  $0.481\%$ ) for different applied fields (between 12 T and 19 T) at 4.2 K and 6.5 K. It is important to underline the large maximum tensile strain ( $0.481\%$ ) of the reversible region. The details about the measurement procedures and results are reported in [7]. In this paper the measurements data are used to calculate the proper fitting parameters for the critical current scaling law [6] that will be used for magnet design and magnet studies. For fitting purpose only the data at 4.2 K were

considered while the data at 6.5 K were used to check the accuracy of the scaling law at different temperatures. Specifically the data at 4.2 K are used to determine the  $s(\varepsilon)$  function that define the upper critical field dependence on the applied strain Eq. (2).

The critical current data were corrected introducing the self-field contribution [8]. Then, for a certain strain, using the measurements at different fields the Kramer field  $B_{c2}^*(4.2 \text{ K}, \varepsilon)$  was determined fitting the data. The Kramer field at different applied strain was than fitted using Eq. (2), Eq. (3), and the  $s(\varepsilon)$  function proposed in the ITER parameterization [6]:

$$s(\varepsilon) = 1 + \frac{C_{a1} \frac{p}{q} \sqrt{e_{sh}^2 + e_{0,a}^2} - \sqrt{(e - e_{sh})^2 + e_{0,a}^2} \frac{q}{p} - C_{a2} \varepsilon}{1 - C_{a1} e_{0,a}} \quad (4)$$

$$e_{sh} = \frac{C_{a2} e_{0,a}}{\sqrt{C_{a1}^2 - C_{a2}^2}} \quad (5)$$

$$\varepsilon = \varepsilon_a - \varepsilon_m \quad (6)$$

where  $\varepsilon_a$  is the applied strain and  $C_{a1}$ ,  $C_{a2}$ ,  $e_{0,a}$ ,  $\varepsilon_m$  the fitting parameters. The fit of the Kramer field is reported in Fig. 3. As expected, the  $s(\varepsilon)$  function proposed in the ITER parameterization fits very well the data for moderate applied strain (Fig. 3 and 4) but it is not accurate for high strain values. Finally using the data at 4.2 K,  $s(\varepsilon)$ ,  $T_{c0max}$  and Eq. (2), the  $B_{c20max}$  was calculated. All the calculated optimal scaling parameters are summarized in Table I.

In order to verify the capability of the scaling law to estimate the critical current at different temperatures, the critical current at 6.5 K was computed using the parameters in Table I and compared with the experimental data, Fig. 5. From the plot one can conclude that in the strain region close to the maximum, the scaling law can estimate quite accurately the critical current at different temperatures. As one could already expect from Fig. 3, the scaling law is not very accurate for large values of applied strain.

### C. Critical and Stability Current Measurements

Critical and stability current measurements were carried out at CERN to study: 1) how much the critical current of this conductor is affected by permanent mechanical deformations; 2) the strand magneto-thermal stability limits. For this purpose a virgin and a rolled strand samples (were measured at 4.3 K and 1.9 K in the magnetic field range between 0 T and 12 T feeding the strand samples with a current up to 2 kA (see Table II). Both V-I and V-H measurements were performed using the procedure described in [9] and [10].

TABLE I SCALING LAW PARAMETERS

$p$	$q$	$C_{a1}$	$C_{a2}$	$e_{0,a}$	$\varepsilon_m$	$T_{c0max}$ K	$B_{c20max}$ [T]
0.453	1.90	60	22	$3.1 \cdot 10^{-3}$	$1.5 \cdot 10^{-3}$	16.3	30.2

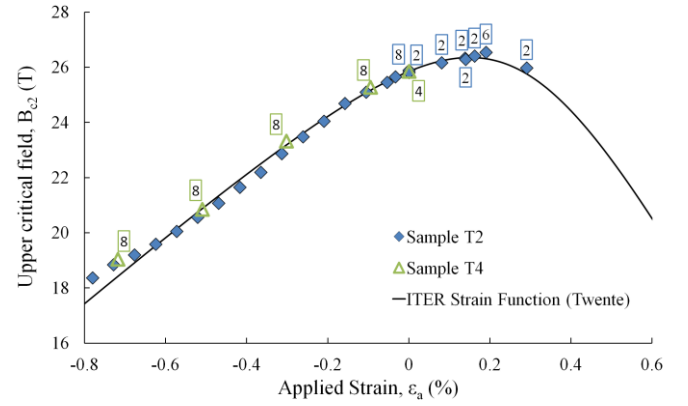


Fig. 3.  $B_{c2}^*$  as a function of the applied strain at 4.2 K calculated from transport current measurements. The values in the text box point out the number of critical current measurement used to extrapolate the  $B_{c2}^*$  for a certain strain; where not indicated, 3  $I_c$  measurements were used.

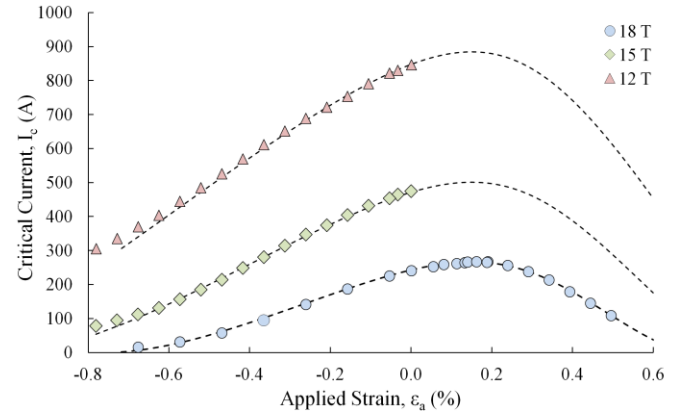


Fig. 4. Critical current as a function of the axial strain at 4.2 K for the sample T2; the dashed lines represent the values calculated using the ITER scaling law [6] and the parameters of Table I.

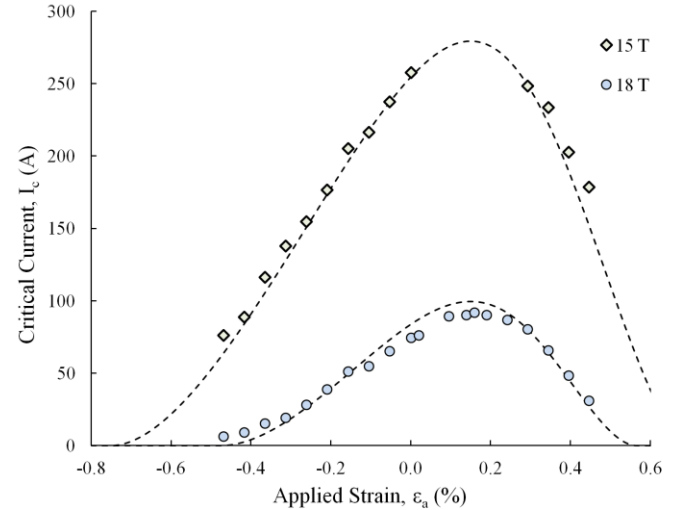


Fig. 5. Critical current as a function of the axial strain at 6.5 K for the sample T5; the dashed lines represent the values calculated using the ITER scaling law [6] and the parameters of Table I.

TABLE II STRAND PROPERTIES

Sample Type	RRR	$I_c(4.3 \text{ K}, 12 \text{ T})$ [A]	$J_c(4.3 \text{ K}, 12 \text{ T})$ [A/mm <sup>2</sup> ]	$B_{c2}^*(4.3 \text{ K})$ [T]
Virgin	235	858	2475	25.5
Rolled 10%	146	839	2422	25.4

\* Determined from critical current measurements at CERN

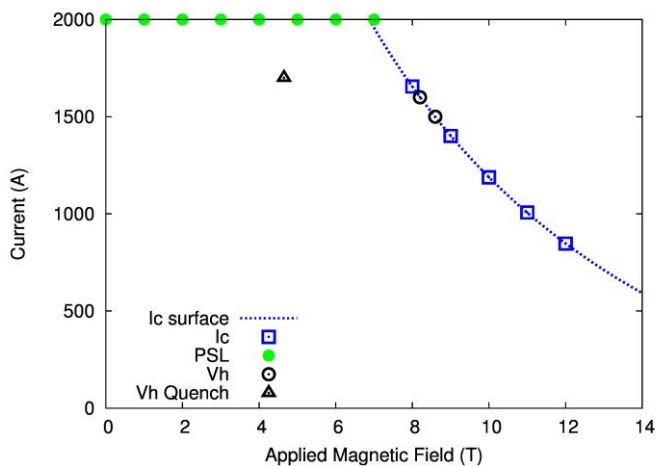


Fig. 6. Critical and quench current at 4.3 K. Unless otherwise stated, the results were obtained via V-I measurements. PSL indicates power supply limit reached without quenching. Vh markers show V-H measurements that reached the strand critical current.

In V-I the sample current is ramped up to quench while keeping constant the applied field. V-H measurements are carried out by ramping the applied field from 0 T to the quench of the sample while keeping constant the current in the sample. Fig. 6 and 7 show the results obtained for the virgin sample respectively at 4.3 K and 1.9 K. For the rolled sample, the results are similar, only a 2% reduction of the  $I_c$  was observed, see Table II. Regarding the conductor stability, at 4.3 K the minimum premature quench current was equal to 1700 A showing that low field instabilities are not an issue for a high field magnet (>12 T) using this conductor.

At 1.9 K, the minimum premature quench current was lower, 1400 A. This quench current was practically obtained at the same field using both V-I and V-H measurements indicating that the self-field instability was the cause of the quench. Indeed premature quenches during V-I measurements are due to the self-field instability while those ones during V-H measurements are due to a combination of self-field and magnetization instability [9], [10].

From the results at 1.9 K one can conclude that low field instability is not a problem for a high field magnet based on this conductor.

Despite a lower RRR, see Table II, the stability performances of the rolled sample were analogous to those of the virgin strand.

In general one can conclude that this conductor has a wide range of operating current available for a high field magnet.

#### IV. CONCLUSION

The 1 mm PIT strand, which is one of the two candidates for building the 13 T FRESKA2 magnet, has been extensively characterized by CERN in collaboration with the University of Geneva. The strand magnetization was measured up to 10.5 T at 4.2 K, 6.5 K and 10 K in a VSM. Critical current versus axial strain measurements were performed at 4.2 K and 6.5 K for different magnetic fields (between 12 T and 19 T) in the reversible region of the applied strain (between -0.785% and 0.481%) using a WASP.

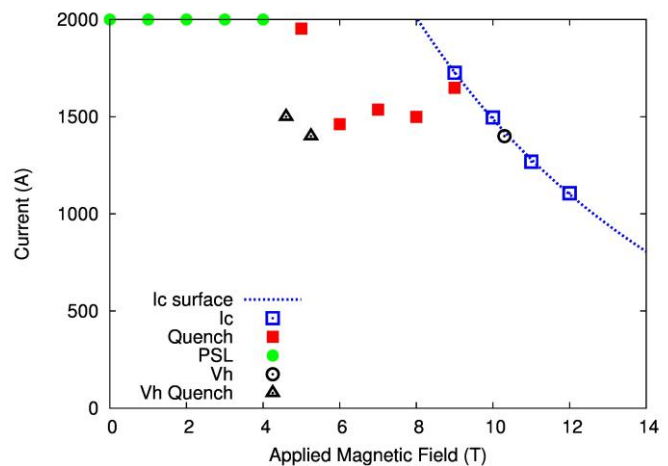


Fig. 7. Critical and quench current at 1.9 K. Unless otherwise stated, the results were obtained via V-I measurements.

These measurements were used to determine the optimal parameters for the critical current that will be used for the magnet design and studies. Finally the critical and stability currents were measured to assess: 1) how much the critical current of this conductor is affected by permanent mechanical deformations; 2) the strand magneto-thermal stability. From these measurements one can conclude that the 1 mm PIT with round sub-elements is a suitable conductor for building the FRESKA2 magnet.

#### ACKNOWLEDGMENTS

The authors would like to acknowledge Florin Buta for the sample heat treatments, Pierre Jacquot, Francis Beauvais, Sebastian Laurent for preparing the samples and Angelo Bonasia for the RRR measurements.

#### REFERENCES

- [1] L. Rossi *et al.*, "Advanced Accelerator Magnets for Upgrading the LHC", submitted to IEEE TAS for publication
- [2] G. de Rijk, "The EuCARD High Field Magnet project", this conference
- [3] M. Karppinen *et al.*, "Design of 11 T Twin-Aperture Nb<sub>3</sub>Sn Dipole Demonstrator Magnet for LHC Upgrades" submitted for publication to *IEEE Trans. Appl. Superconduct.*
- [4] A. Milanese *et al.*, "Design of the EuCARD high field model dipole magnet FRESKA2", submitted for publication to *IEEE Trans. Appl. Superconduct.*
- [5] J. C. Perez *et al.*, "The SMC (Short Model Coil) dipole: An R&D program for Nb<sub>3</sub>Sn accelerator magnets", submitted for publication to *IEEE Trans. Appl. Superconduct.*
- [6] L. Bottura, B. Bordini, " $J_c(B, T, \epsilon)$  Parameterization for the ITER Nb<sub>3</sub>Sn Production", *IEEE Trans. Appl. Superconduct.*, 19, no. 3, pp. 1521-1524, June 2009
- [7] G. Mondonico *et al.*, "Critical Current response under axial and transverse stress of new generation PIT Nb<sub>3</sub>Sn wires", presented at this conference
- [8] B. Bordini, "Self-Field Correction in Critical Current Measurements of Superconducting Wires Tested on ITER VAMAS Barrels", *CERN Internal Note*, EDMS Nr: 1105765, November 2010
- [9] B. Bordini, E. Barzi, S. Feher, L. Rossi, and A. V. Zlobin, "Self-field effects in magneto-thermal instabilities for Nb-Sn strands," *IEEE Trans. Appl. Supercond.* vol. 18, no. 2, pp. 1309 - 1312, Jun. 2008.
- [10] B. Bordini B, L. Rossi, "Self field instability in high  $J_c$  Nb<sub>3</sub>Sn strands with high copper residual resistivity ratio," *IEEE Trans. Appl. Supercond.* vol. 19 no. 3, pp. 2470-2476, June 2009.